J|A|C|S ARTICLES

Published on Web 11/11/2010

Transfer of a Disilenyl Moiety to Aromatic Substrates and Lateral Functional Group Transformation in Aryl Disilenes

Jonathan Jeck,[†] Iulia Bejan,[†] Andrew J. P. White,[†] Dominik Nied,[‡] Frank Breher,*[,‡] and David Scheschkewitz*[,†]

Department of Chemistry, Imperial College, London SW7 2AZ, United Kingdom, and Institute of Inorganic Chemistry, Karlsruhe Institute of Technology (KIT), 76131 Karlsruhe, Germany

Received September 1, 2010; E-mail: breher@kit.edu; d.scheschkewitz@imperial.ac.uk

Abstract: The reaction of 1 equiv of the disilenide $Tip_2Si{=}Si(Tip)Li$ (**5**; Tip = 2,4,6-$^i Pr_3C_6H_2$) with para-substituted phenyl iodides, 4-X-PhI, transfers the $Tip_2Si{=}Si(Tip)$ moiety with elimination of lithium iodide to yield the laterally functionalized disilenes $Tip_2Si{=}Si(Tip)$(4-X-Ph) [X = H (**6a**), F (**6b**), Cl (**6c**), Br (**6d**), I (**6e**)]. The UV−vis absorptions of **6a**−**d** suggest a linear correlation with electronic Hammett parameters. In addition, X-ray structural analyses of **6a**−**d** verified the theoretically predicted linear dependence of the Si=Si bond length and trans-bent angles. The *p*-bromophenyl-substituted disilene **6d** undergoes a metal−halogen exchange reaction to give **6f** (X = Li), which was trapped with Me_3SiCl to afford **6g** (X = $SiMe_3$). In the case of simple phenyl halides PhX without additional functionality, the reaction with **5** proceeded smoothly for X = Br, but phenyl chlorides and fluorides did not react at room temperature even after one week, hinting at an S_N2-type aromatic substitution mechanism. Reactions of *p*- and *m*-diiodobenzene with **5** afford the corresponding phenylene-bridged tetrasiladienes *p*-**7** and *m*-**7**. While red *p*-**7** (λ_{max} = 508 nm) exhibits efficient conjugation of the two Si=Si bonds with the phenylene linker, the conjugation in yellow *m*-**7** (λ_{max} = 449 nm) is much less effective. Electrochemical studies of *m*-**7** and *p*-**7** as well as density functional theory calculations and electron paramagnetic resonance studies of their respective radical anions provided further support for the notion of conjugation.

1. Introduction

Compounds with Si=Si double bonds have continued to attract much interest ever since the seminal report by West, Fink, and Michl on the isolation of the first stable example, disilene **1** (Chart 1).[1,2] In comparison with alkenes, disilenes are distinguished by considerably smaller HOMO−LUMO gaps, which is a manifestation of the relatively weak π bonding between heavier main-group elements.[2] In addition, the comparatively high polarizability of silicon relative to carbon results in shallow energy profiles for distortions of the Si=Si bond that diminish the orbital overlap and thus the HOMO−LUMO gap of disilenes.

For example, steric repulsion between the substituents of the blue disilene **2a** gives rise to strongly twisted trigonal-planar coordination environments of the doubly bonded silicon atoms (the twist angle, τ, is 54°),[3a] while the sterically less encumbered yellow disilene **2b** is almost perfectly planar.[3b] Similarly, the more pronounced ring strain in red *trans*-**3** causes much larger trans bending and twisting in comparison with the yellow isomer *cis*-**3**, which explains the greater red shift of the longest-wavelength UV−vis absorption of *trans*-**3**.[4] Even energetically weak parameters such as crystal packing forces affect the solid-state structures: disilene **1** crystallizes in a planar, slightly twisted, or trans-bent conformation of the Si=Si bond, depending on the presence and nature of the cocrystallized solvent.[5]

In order to exploit the markedly different chemical and physical properties of disilenes relative to alkenes, the incor-

Chart 1. Stable Disilenes Illustrating the Conformational Flexibility of the Si=Si Bond[a]

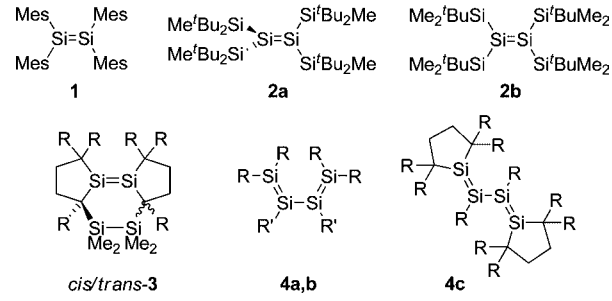

[a] In **1**, Mes = 2,4,6-$Me_3C_6H_2$. In *cis*/*trans*-**3**, R = $SiMe_3$. In **4a**, R = R′ = Tip = 2,4,6-$^i Pr_3C_6H_2$. In **4b**, R = Si^{t}Bu$_2$Me, R′ = Mes. In **4c**, R = $SiMe_3$.

[†] Imperial College.
[‡] Karlsruhe Institute of Technology.

(1) West, R.; Fink, M. J.; Michl, J. *Science* **1981**, *214*, 1343.
(2) Recent reviews: (a) Scheschkewitz, D. *Chem.—Eur. J.* **2009**, *15*, 2476. (b) Kira, M.; Iwamoto, T. *Adv. Organomet. Chem.* **2006**, *54*, 73. (c) Lee, V. Y.; Sekiguchi, A. *Organometallics* **2004**, *23*, 2822. (d) Weidenbruch, M. *Angew. Chem.* **2003**, *115*, 2322; *Angew. Chem., Int. Ed.* **2003**, *42*, 2222. (e) Sekiguchi, A.; Lee, V. Y. *Chem. Rev.* **2003**, *103*, 1429. (f) West, R. *Polyhedron* **2002**, *21*, 467. (g) Weidenbruch, M. *J. Organomet. Chem.* **2002**, *646*, 39. (h) Kira, M. *Pure Appl. Chem.* **2000**, *72*, 2333.
(3) (a) Sekiguchi, A.; Inoue, S.; Ichinohe, M.; Arai, Y. *J. Am. Chem. Soc.* **2004**, *126*, 9626. (b) Kira, M.; Maruyama, T.; Kabuto, C.; Ebata, K.; Sakurai, H. *Angew. Chem.* **1994**, *106*, 1575; *Angew. Chem., Int. Ed. Engl.* **1994**, *33*, 1489.
(4) Tanaka, R.; Iwamoto, T.; Kira, M. *Angew. Chem.* **2006**, *118*, 6519; *Angew. Chem., Int. Ed.* **2006**, *45*, 6371.

10.1021/ja107547s

poration of Si═Si moieties into π-conjugated systems is particularly interesting. In this context, a few tetrasilabutadienes, **4a**−**c**, have been synthesized and used to demonstrate that the well-known red shift associated with an extension of the conjugation path length in carbon systems is significant in all-silicon systems as well.[6] In light of the importance of semiconducting π-conjugated organic polymers, in which a variety of supplementary linking units alternate with the C═C double bonds,[7] we decided to investigate the effects of conjugation between such carbon-based linking units and Si═Si bonds. Such endeavors seemed particularly worthwhile in view of the fact that the groups of Gates, Protasiewicz, and more recently Ott have reported substantial progress with such an approach in the case of P═C and P═P bonds, including the synthesis of polymeric systems.[8,9]

In comparison with phosphorus-containing double bonds, however, the synthetic options for the generation of Si═Si bonds are limited,[2] and functionalized derivatives have been unknown until recently, except for a few cases mentioned in passing in the literature.[6a,10] Consequently, in the past few years, considerable effort has been devoted to the synthesis of disilenes with nucleophilic[11,6b] or electrophilic[12] functionality. In all cases, the functional group is directly attached to the silicon atom(s) of the Si═Si bond. In reactions with aryl halides, disilenides (i.e., disila analogues of vinyllithiums) are able to transfer the Si═Si moiety to aromatic substrates.[13a,11f] *p*-Phenylene-bridged tetrasiladienes were obtained in nearly quantitative spectroscopic yield using this method,[13a] while a more conventional approach via reductive coupling of halosilanes produced complicated product mixtures from which the desired phenylene-bridged tetrasiladienes were isolated by chromatographic techniques in comparatively low yield.[13b]

Scheme 1. Syntheses of Para-Functionalized Phenyldisilenes **6a**−**e** and Phenylene-Bridged Tetrasiladienes *p*-**7** and *m*-**7**[a]

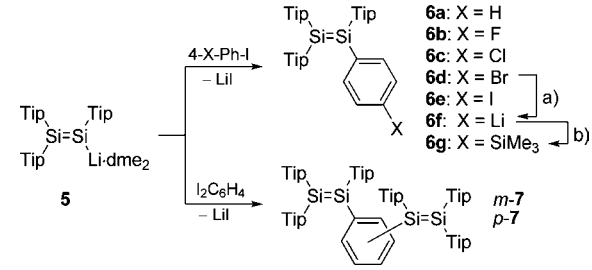

[a] Abbreviations: dme = 1,2-dimethoxyethane, Tip = 2,4,6-^{i}Pr$_3$C$_6$H$_2$). Conditions: (a) −80 °C, 2 ^{t}BuLi; (b) −80 °C, Me$_3$SiCl.

The present study concerns the elucidation of the scope of the Si═Si transfer to aryl halides effected by nucleophilic disilenides with respect to (1) different halide leaving groups, (2) the compatibility with residual lateral functionalities and functional group transformations at the periphery of the Si═Si bond, and (3) the multiple transfer of Si═Si moieties and the electronic communication mediated by the different phenylene linkers.

2. Results and Discussion

As part of our investigations into the reactivity of disilenide **5** toward organic substrates,[14] we recently reported that the reactions of **5** with iodobenzene and 1,4-diiodobenzene furnish the phenyl-substituted disilene **6a** (X = H) and the *p*-phenylene-bridged tetrasiladiene *p*-**7**, respectively.[13a] Here we show that the same methodology can be used for the preparation of the *m*-phenylene-bridged derivative *m*-**7** (Scheme 1). In addition, we have found that **6a** can alternatively be prepared from **5** and bromobenzene (in place of the more expensive iodobenzene) but not from fluoro- or chlorobenzene. Taking advantage of the strongly differing relative reaction rates, we have also synthesized phenyl-substituted disilenes **6b**−**d** featuring residual halogen atoms X (**6b**, X = F; **6c**, X = Cl; **6d**, X = Br) as lateral functionalities at the para positions of the newly introduced phenyl groups (Scheme 1). All of these compounds were completely characterized by means of multinuclear NMR and UV−vis spectroscopy as well as mass spectrometry. Additionally, single-crystal X-ray diffraction studies allowed us to establish a direct correlation between the trans-bent angles and the Si═Si bond length, which are theoretically interdependent. Finally, the reaction of **6d** with ^{t}BuLi to afford para-lithiated **6f** serves as a proof of principle that functional group transformation on the aromatic periphery of disilenes is possible despite the high reactivity of the Si═Si moiety.

2.1. Treatment of Disilenide 5 with Halobenzenes PhX (X = F, Cl, Br, I). As we recently reported, disilenide **5** reacts with iodobenzene to afford phenyldisilene **6a** in an essentially quantitative manner.[13a] This formal nucleophilic aromatic substitution in the absence of a transition-metal catalyst proceeds with surprising ease and selectivity. The possibly best known reaction mechanism of nucleophilic aromatic substitution reactions is referred to as S$_N$Ar and involves the anionic Meisen-

(5) (a) Fink, M. J.; Michalczyk, M. J.; Haller, K. J.; Michl, J.; West, R. *Organometallics* **1984**, *3*, 793. (b) Wind, M.; Powell, D. R.; West, R. *Organometallics* **1996**, *15*, 5772.
(6) (a) Weidenbruch, M.; Willms, S.; Saak, W.; Henkel, G. *Angew. Chem.* **1997**, *109*, 2612; *Angew. Chem., Int. Ed. Engl.* **1997**, *36*, 2503. (b) Ichinohe, M.; Sanuki, K.; Inoue, S.; Sekiguchi, A. *Organometallics* **2004**, *23*, 3088. (c) Uchiyama, K.; Nagendran, S.; Ishida, S.; Iwamoto, T.; Kira, M. *J. Am. Chem. Soc.* **2007**, *129*, 10638.
(7) A recent review: Coropceanu, V.; Cornil, J.; da Silva Filho, D. A.; Olivier, Y.; Silbey, R.; Brédas, J.-L. *Chem. Rev.* **2007**, *107*, 926.
(8) (a) Wright, V. A.; Gates, D. P. *Angew. Chem.* **2002**, *114*, 2495; *Angew. Chem., Int. Ed.* **2002**, *41*, 2389. (b) Smith, R. C.; Protasiewicz, J. D. *Eur. J. Inorg. Chem.* **2004**, 998. (c) Wright, V. A.; Patrick, B. O.; Schneider, C.; Gates, D. P. *J. Am. Chem. Soc.* **2006**, *128*, 8836. (d) Geng, X.-L.; Ott, S. *Chem. Commun.* **2009**, 7206. (e) Geng, X.-L.; Hu, Q.; Schäfer, B.; Ott, S. *Org. Lett.* **2010**, *12*, 692. (f) Washington, M. P.; Gudimetla, V. B.; Laughlin, F. L.; Deligonul, N.; He, S.; Payton, J. L.; Simpson, M. C.; Protasiewicz, J. D. *J. Am. Chem. Soc.* **2010**, *132*, 4566.
(9) Smith, R. C.; Protasiewicz, J. D. *J. Am. Chem. Soc.* **2004**, *126*, 2268.
(10) (a) Wiberg, N.; Niedermayer, W.; Fischer, G.; Nöth, H.; Suter, M. *Eur. J. Inorg. Chem.* **2002**, 1066. (b) Wiberg, N.; Vasisht, S. K.; Fischer, G.; Mayer, P. *Z. Anorg. Allg. Chem.* **2004**, *630*, 1823.
(11) (a) Scheschkewitz, D. *Angew. Chem.* **2004**, *116*, 3025; *Angew. Chem., Int. Ed.* **2004**, *43*, 2965. (b) Inoue, S.; Ichinohe, M.; Sekiguchi, A. *Chem. Lett.* **2005**, *34*, 1564. (c) Abersfelder, K.; Güclü, D.; Scheschkewitz, D. *Angew. Chem.* **2006**, *118*, 1673; *Angew. Chem., Int. Ed.* **2006**, *45*, 1643. (d) Kinjo, R.; Ichinohe, M.; Sekiguchi, A. *J. Am. Chem. Soc.* **2007**, *129*, 26. (e) Ichinohe, M.; Sanuki, K.; Inoue, S.; Sekiguchi, A. *Silicon Chem.* **2007**, *3*, 111. (f) Iwamoto, T.; Kobayashi, M.; Uchiyama, K.; Sasaki, S.; Nagendran, S.; Isobe, H.; Kira, M. *J. Am. Chem. Soc.* **2009**, *131*, 3156.
(12) (a) Sasamori, T.; Hironaka, K.; Sugiyama, Y.; Takagi, N.; Nagase, S.; Hosoi, Y.; Furukawa, Y.; Tokitoh, N. *J. Am. Chem. Soc.* **2008**, *130*, 13856. (b) Hartmann, M.; Haji-Abdi, A.; Abersfelder, K.; Haycock, P. R.; White, A. J. P.; Scheschkewitz, D. *Dalton Trans.* **2010**, *39*, 9288.
(13) (a) Bejan, I.; Scheschkewitz, D. *Angew. Chem.* **2007**, *119*, 5885; *Angew. Chem., Int. Ed.* **2007**, *46*, 5783. (b) Fukazawa, A.; Li, Y.; Yamaguchi, S.; Tsuji, H.; Tamao, K. *J. Am. Chem. Soc.* **2007**, *129*, 14164.
(14) (a) Bejan, I.; Güclü, D.; Inoue, S.; Ichinohe, M.; Sekiguchi, A.; Scheschkewitz, D. *Angew. Chem.* **2007**, *119*, 3413; *Angew. Chem., Int. Ed.* **2007**, *46*, 3349. (b) Bejan, I.; Inoue, S.; Ichinohe, M.; Sekiguchi, A.; Scheschkewitz, D. *Chem.—Eur. J.* **2008**, *14*, 7119.

Scheme 2. Reactivity of Halobenzenes PhX toward Disilenide **5** (X = F, Cl, Br, I; Tip = 2,4,6-$^{i}Pr_3C_6H_2$)

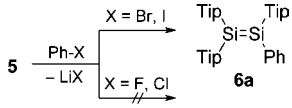

heimer complex as a reactive intermediate.[15] Because the stability of this complex is rate-determining in S_NAr reactions, better leaving groups (which decrease the stability of the complex) slow down the reaction. Consequently, the rate of S_NAr reactions increases with decreasing leaving tendency of the halogen substituent: I < Br ≪ Cl < F.[15] In order to gather mechanistic information on the Si═Si transfer reaction in this regard and to explore its preparative potential, we treated samples of disilenide **5** in C_6D_6 with different halobenzenes at room temperature (Scheme 2).

Indeed, we found that bromobenzene reacts with **5** as cleanly as iodobenzene whether used stoichiometrically or in excess. The smooth reactions of both bromo- and iodobenzene with **5** and the absence of detectable traces of the homocoupling products [tetrasilabutadiene (**4a**) and biphenyl] renders stepwise mechanistic options (i.e., initial metal−halogen exchange or single-electron redox processes) unlikely in the present case. Conversely, Weidenbruch et al.[6a] had explained the formation of **4a** upon treatment of in situ-generated **5** with 0.5 equiv of the more encumbered MesBr (Mes = 2,4,6-$Me_3C_6H_2$) in 1,2-dimethoxyethane in terms of an initial metal−halogen exchange followed by salt elimination between the thus-formed bromodisilene and residual disilenide **5**. Despite the potential preparative problems that the competing formation of **4a** may thus cause with sterically more demanding substrates, the larger number and lower price of commercially available bromoarenes significantly extends the potential scope of the Si═Si transfer reaction using **5**.

In contrast to the cases of bromo- and iodobenzene, no reaction at all was observed after one week at room temperature using either fluoro- or chlorobenzene, even in the presence of a 10-fold excess of the halobenzene; not even trace amounts of phenyldisilene **6a** were detected in either experiment. The stability of **5** in the presence of both of these reagents excludes the S_NAr mechanism for the Si═Si transfer reaction. If the S_NAr mechanism were active, the reaction with aryl fluorides should be the most rapid. On this basis, we favor an S_N2-like aromatic substitution mechanism for the reaction of disilenide **5** with simple, sterically uncluttered aryl halides. The alternative of a radical chain mechanism of the $S_{RN}Ar$ type appears to be unlikely in view of the reactivity of **5** with dihalobenzenes (see below).

2.2. Reactions of Disilenide 5 with 1-Iodo-4-halobenzenes 4-XPhI (X = F, Cl, Br, I). In our earlier communication, we described the reaction of 2 equiv of disilenide **5** with 1,4-diiodobenzene, which quantitatively affords the *p*-phenylene-bridged compound *p*-**7**.[13a] In an attempt to obtain a disilene with a para-functionalized phenyl substituent and in order to elucidate the relative reaction rates of the first and second substitution steps, we reacted 1,4-diiodobenzene with just 1 equiv of **5** (Scheme 3). Despite the use of a precise 1:1 stoichiometry, the anticipated monosubstitution product **6e** could be obtained only with ∼10% *p*-**7** and 10% unreacted 1,4-diiodobenzene.

Scheme 3. Synthesis of Para-Functionalized Phenyldisilenes **6a**−**e** (Tip = 2,4,6-$^{i}Pr_3C_6H_2$)

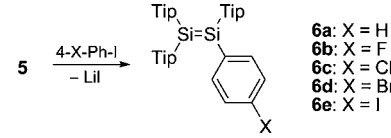

The predominant formation of **6e** nonetheless provides additional support for an S_N2-like aromatic substitution mechanism, although the second substitution indeed takes place with a competitive rate even in the presence of undoubtedly increasing steric congestion. As demonstrated by Bunnett,[16] $S_{RN}Ar$-type reactions of diiodobenzenes with diethylphosphite tend to afford the disubstitution product exclusively. However, we cannot completely rule out the formation of an initial encounter complex that may undergo electron transfer to form a solvent-cage-stabilized radical pair prior to product formation.[17]

From a more preparative viewpoint, the strongly differing reactivity of different halobenzenes offers a possible solution to the above-mentioned selectivity problem. We therefore decided to investigate the reactions of **5** with dihalobenzenes featuring two differing halogens. Indeed, the reactions of **5** with 1-iodo-4-halobenzenes, 4-XPhI, in benzene at room temperature proceeded cleanly to afford exclusively the products **6b**−**d** corresponding to substitution at the iodo position (Scheme 3). Except for **6e**, the *p*-halophenyl-substituted disilenes were stable at room temperature in the absence of air and moisture. Despite the essentially quantitative conversions to **6b**−**d** as determined by NMR spectroscopy, the isolated yields of the products suffered from the increasing solubility in hydrocarbons in going from **6b** to **6d** (**6b**, 86%; **6c**, 47%; **6d**, 23%). All of the isolated *p*-halophenyl-substituted disilenes **6b**−**d** (**6e** could not be isolated) were completely characterized by multinuclear NMR spectroscopy and single-crystal X-ray diffraction. Table 1 summarizes and compares selected spectroscopic and structural parameters.

The ^{29}Si NMR resonances of **6b**−**e** (Table 1) are very similar to those of **6a**, indicating a rather weak perturbation of the Si═Si π bonding by the halogen atom at the para position of the phenyl substituent. As pointed out by Strohmann, Kaupp, and coworkers,[18] the ^{29}Si NMR shifts in multiply bonded silicon species are very sensitive indicators of electronegativity differences in the substituents. Even though the longest-wavelength absorptions in the UV−vis spectra of **6a**−**d** obtained in hexane (Table 1) are also only slightly perturbed, as evidenced by the small red shift from X = F to X = Br, a positive linear correlation with the modified Hammett parameter σ_{P+} (as introduced by Brown and Okamoto[19]) is evident (Figure 1). As it is strictly empirical in nature, such a Hammett equation does not lend itself to ready interpretation but might be useful for the prediction of the HOMO−LUMO gap of derivatives yet to be synthesized. It should be kept in mind, however, that it is common practice to apply different equations for different subsets of functional groups with similar electronic properties.[20]

(15) Review: Terrier, F. *Chem. Rev.* **1982**, *82*, 77.
(16) Review: Bunnett, J. F. *Acc. Chem. Res.* **1978**, *11*, 413.
(17) For example, hydrometalation of conjugated dienes with complex iron hydrides is known to proceed via a radical-pair mechanism. See: Shackleton, T. A.; Baird, M. C. *Organometallics* **1989**, *8*, 2225.
(18) (a) Auer, D.; Strohmann, C.; Arbuznikov, A. V.; Kaupp, M. *Organometallics* **2003**, *22*, 2442. (b) Auer, D.; Kaupp, M.; Strohmann, C. *Organometallics* **2005**, *24*, 6331.
(19) Brown, H. C.; Okamoto, Y. *J. Am. Chem. Soc.* **1958**, *80*, 4979.
(20) Ušćumlić, G. S.; Mijin, D. Ž.; Valentić, N. V.; Vajs, V. V.; Sušić, B. M. *Chem. Phys. Lett.* **2004**, *397*, 148.

Table 1. NMR and UV−Vis Spectroscopic Parameters and Structural Parameters of Para-Functionalized Phenyldisilenes **6a**−**e** and Phenylene-Bridged Tetrasiladienes *p*-**7** and *m*-**7**

	6a[a]	6b	6c	6d	6e	*p*-7[a]	*m*-7
δ^{29}Si1 (ppm)[b]	71.8	70.6	69.3	69.2	69.7[d]	70.7	72.9
δ^{29}Si2 (ppm)[c]	55.2	55.7	57.3	57.4	57.9[d]	56.8	54.6
^1J(Si1,Si2) (Hz)	151.4	[f]	[f]	[f]	[f]	150.0	148.4
d(Si1,Si2) (Å)	2.175(1)[f]	2.147(1)[f]	2.1735(4)	2.1707(5)	−	2.1674(8)	2.189(1)[g]
θ_{Si1} (deg)[d]	22.8[g]	5.5[g]	15.8	16.2	−	16.5	20.3[g]
θ_{Si2} (deg)[d]	22.0[g]	5.9[g]	23.8	24.5	−	19.3	26.7[g]
τ (deg)[e]	5.0[g]	5.4[g]	10.8	10.6	−	3.4	10.6[g]
λ_{max} (nm)	439	437	445	447	−	508	450
ε (10^3 M^{-1} cm^{-1})	19	16.8	19.2	16.2	−	27	39

[a] Data from ref 13a. [b] SiTip. [c] $SiTip_2$. [d] Trans-bent angle [$\theta_{SiX} = 90° -$ (angle between the Si1−Si2 vector and the normal to the plane defined by SiX and the pendant substituents)]. [e] Twist angle (τ is the angle between the normals to two planes, each of which is defined by one of the silicon atoms and the pendant substituents). [f] Not observed. [g] Average value.

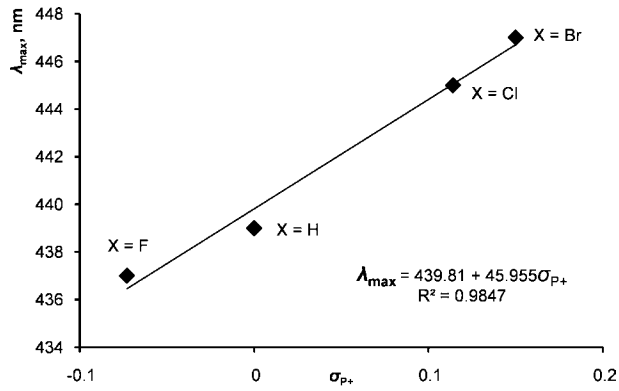

Figure 1. Linear correlation (Hammett equation) between λ_{max} for the longest-wavelength absorptions of **6a**−**d** and the electronic Hammett parameter σ_{P+} for the para substituent X.

In order to clarify whether the halogen atom at the para position of **6b**−**d** affects the solid-state structure as well, we carried out X-ray diffraction studies on single crystals of the entire series [Table 1 and Figure 2; crystallographic data are summarized in Table 2 (in the Experimental Section) as well as in the Supporting Information]. The structure of **6a** was reported in our previous communication[13a] and is included for comparison. All of the phenyl-substituted disilenes crystallized in monoclinic space groups (**6a** and **6b**, $P2_1$; **6c** and **6d**, $P2_1/c$).

As previously observed for the chlorosilyl-substituted disilene $Ph_2ClSi(Tip)Si{=}SiTip_2$ (**8**),[21] the *p*-fluorophenyl derivative **6b** crystallizes with four crystallographically independent molecules in the asymmetric unit. As a consequence of the usual conformational flexibility of the Si═Si bond,[2] the four independent molecules of **6b** vary significantly in their pertinent structural features, namely, the trans-bent angles (θ_{Si1} = 2.8−8.1°), the twist angles (τ = 2.6−8.3°), and the Si−Si bond lengths [d(Si1,Si2) = 2.1417(1)−2.1536(1) Å]. Nevertheless, unlike in the case of **6a**, where considerable trans bending was observed,[13a] **6b** appears to have a preference for more planar conformations, since three of the four independent molecules exhibit rather small trans-bent angles close to planarity (Table 1).

The *p*-chloro- and *p*-bromophenyl derivatives **6c** and **6d**, respectively, crystallize in isomorphous and hence very similar structures. Both exhibit relatively high trans-bent angles and long Si═Si distances (Table 1). The finding that *p*-fluorophenyl-substituted disilene **6b** appears to prefer a more planar Si═Si bond conformation seemingly contradicts the bonding model for multiple bonding in heavier alkene homologues developed by Carter, Goddard, Malrieu, and Trinquier (the CGMT model): the *p*-fluorophenyl substituent should stabilize the singlet state of the corresponding silylene fragment through inductive and mesomeric effects. As had been pointed out by Power and coworkers[22] in the context of distannynes, however, the shallowness of the relevant potential energy surface must be kept in mind in any discussions of substituent effects. Nonetheless, some general conclusions with respect to the interrelation of bond length and trans bending are warranted. The CGMT model predicts a weakening of the Si═Si bond as the extent of trans bending increases.[23,24] In a more practical approach, Karni and Apeloig[25] computationally established linear relationships between the three observable parameters (the Si═Si bond length

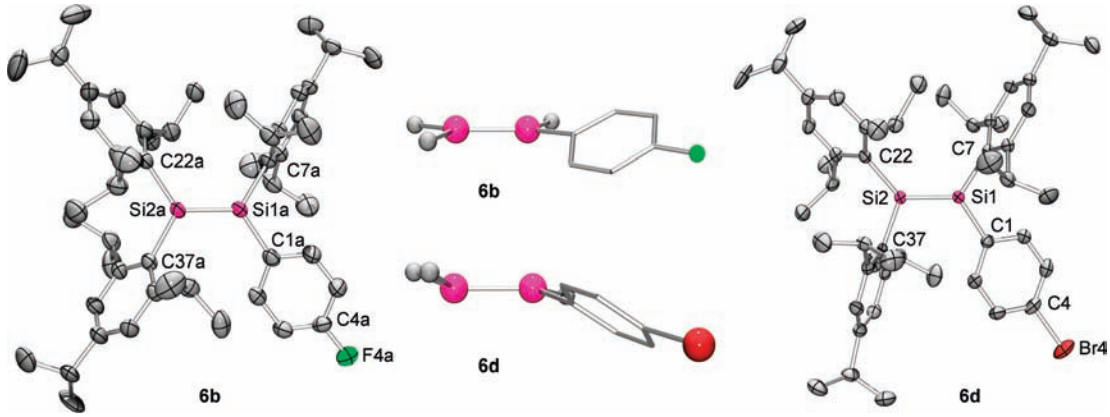

Figure 2. Molecular structures of (left) one of the four crystallographically independent molecules in the crystal structure of *p*-fluorophenyldisilene **6b** and (right) *p*-bromophenyldisilene **6d**. Hydrogen atoms and alternative positions of disordered isopropyl groups have been omitted for clarity. The ball-and-stick representations at the center show simplified side views of the molecules.

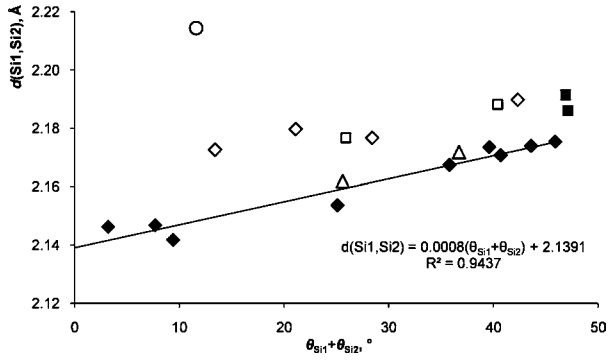

Figure 3. Linear correlation between the sum of the trans-bent angles $\theta_{Si1} + \theta_{Si2}$ and the Si=Si bond distance for **6a**−**d** and *p*-**7** (◆). Data points for *m*-**7** (■) were not considered for linear regression. Data for disilenes **8** (◇), **9** (□), **10** (△), and **11** (○) are included for comparison.

and the two trans-bent angles θ) and the sum of the two singlet−triplet gaps of the constitutent silylene fragments, $\sum\Delta E_{S-T}$. Although they did not explicitly mention it, this result also implies a linear correlation between the two dependent observables, namely, the bond length and the trans-bent angles θ. This has been qualitatively confirmed by experiment numerous times,[2] but a quantitative experimental correlation has not been reported to date, presumably because of the various other interfering factors that reduce comparability (e.g., differing steric bulk). With a number of examples now in hand (i.e., **6a**−**d** and *p*-**7**) where these interfering factors are conceivably negligible, such a correlation can be envisaged. Indeed the R^2 value of 0.9437 for the plot of the Si=Si bond length of the crystallographically independent disilene molecules against the sum of the trans-bent angles (Figure 3) indicates a linear relationship. Individual plots of the θ values against the Si=Si distance correlate less well, presumably because of the non-negligible influence of packing forces on the molecular geometry, which is apparent from the very fact that four significantly different geometries are encountered in the solid state of **6b**. The much better correlation between *d*(Si1,Si2) and the sum of the angles $\theta_{Si1} + \theta_{Si2}$ as shown in Figure 3, illustrates that despite the conformational freedom of disilenes, the overall interdependence of the trans-bent angles and the Si=Si distance is maintained. Incidentally, the intercept with the ordinate at 2.1391 Å corresponds nicely to the Si=Si bond length of the essentially planar disilene $Tip_2Si{=}SiTip_2$ (2.144 Å).[26]

The amount of deviation from the empirical equation [$d(Si1,Si2) = 0.008(\theta_{Si1} + \theta_{Si2}) + 2.1391$] may serve as a convenient indicator that the presence of electronic or steric effects affect the bond length of the Si=Si bonds of the $Tip_2Si{=}Si(Tip)R$ type. Indeed, the inclusion of the previously reported data for $Tip_2Si{=}Si(Tip)_2Cl$ (**8**),[21] $Tip_2Si{=}Si(Tip)$-$SiPhSn^tBu_2Cl$ (**9**),[27] $Tip_2Si{=}Si(Tip)SnMe_3$ (**10**),[27] and $Tip_2Si{=}Si$-(Tip)$ZrCp_2Cl$ (**11**)[28] into the graph serves as proof of principle: only the sterically and electronically comparatively innocuous trimethylstannyldisilene **10** nicely fits the linear regression. For **8** and **9**, a combination of both steric and electronic effects had been invoked to explain the relatively long Si=Si bond,[21,27] whereas the Si=Si bond in **11** interacts with the adjacent zirconium and is strongly twisted, which results in a significant perturbation.[28]

Scheme 4. Metal−Halogen Exchange Reaction of **6d** and Trapping of *p*-Lithiophenyl-Substituted Disilene **6f** with Me_3SiCl To Form a Mixture of **6g** and **6a** (Tip = 2,4,6-$^i Pr_3C_6H_2$)

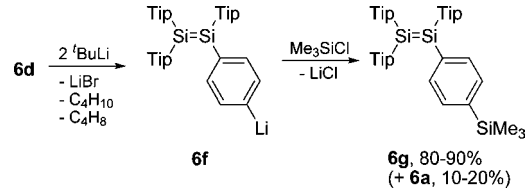

2.3. Metal−Halogen Exchange Reaction of *p*-Bromophenyldisilene 6d. Reactivity studies of disilenes in the past mainly concerned the Si=Si double bond itself.[2] As mentioned in the Introduction, recent efforts have made available directly Si-functionalized disilenes.[6a,b,11,12] To the best of our knowledge, however, functional group transformations at the periphery of Si=Si moieties have not been reported to date. With the para-functionalized phenyldisilenes in hand, we investigated the metal−halogen exchange reaction of the *p*-bromophenyl-substituted derivative **6d**.

Indeed, treatment of **6d** with 2 equiv of ^{t}BuLi at −80 °C followed by intermittent warming to −50 °C for 1 h and subsequent treatment with 1.05 equiv of Me_3SiCl afforded a product that on the basis of the NMR spectroscopic data was tentatively identified as a mixture of *p*-trimethylsilylphenyldisilene **6g** and the product of protonation of **6f**, namely, phenyldisilene **6a** (Scheme 4). In different runs we obtained **6g**/**6a** ratios between 8:2 and 9:1. Since all attempts to separate these mixtures by crystallization failed, we synthesized **6g** in similar purity by the independent route of reacting disilenide **5** with 1 equiv of *p*-trimethylsilylbromobenzene in order to prove its constitution. The identity of the multinuclear NMR spectroscopic data of the products of these two independent syntheses unambiguously proved the formation of **6g** and thus the formation of *p*-lithiophenyldisilene **6f** in the reaction of **6d** with ^{t}BuLi.

2.4. Reactions of Disilenide 5 with Diiodobenzenes. In order to lend further support to the hypothesis that the pronounced red shift in the UV−vis spectrum of the *p*-phenylene-bridged tetrasiladiene *p*-**7** is truly due to conjugation effects, we chose to investigate the corresponding meta derivative, *m*-**7**. It is well-established that *m*-phenylene linking units interrupt the conjugation pathway and therefore the electronic communication in conjugated systems.[29]

Reaction of 2 equiv of disilenide **5** with *m*-diiodobenzene following the established protocol indeed yielded the desired product *m*-**7** quantitatively (Scheme 5). The absence of a significant color change during the reaction already suggested much less effective conjugation at this early stage of the study. Crystallization from a minute amount of benzene afforded *m*-**7**

(21) Abersfelder, K.; Scheschkewitz, D. *J. Am. Chem. Soc.* **2008**, *130*, 4114.
(22) Fischer, R. C.; Pu, L.; Fettinger, J. C.; Brynda, M. A.; Power, P. P. *J. Am. Chem. Soc.* **2006**, *128*, 11366.
(23) (a) Carter, E. A.; Goddard, W. A., III. *J. Phys. Chem.* **1986**, *90*, 998. (b) Trinquier, G.; Malrieu, J.-P. *J. Am. Chem. Soc.* **1987**, *109*, 5303. (c) Malrieu, J.-P.; Trinquier, G. *J. Am. Chem. Soc.* **1989**, *111*, 5916.
(24) Reviews of the CGMT model: (a) Driess, M.; Grützmacher, H. *Angew. Chem.* **1996**, *108*, 900; *Angew. Chem., Int. Ed. Engl.* **1996**, *35*, 828. (b) Grützmacher, H.; Fässler, T. F. *Chem.−Eur. J.* **2000**, *6*, 2317.
(25) Karni, M.; Apeloig, Y. *J. Am. Chem. Soc.* **1990**, *112*, 8589.
(26) Watanabe, H.; Takeuchi, K.; Fukawa, N.; Kato, M.; Goto, M.; Nagai, Y. *Chem. Lett.* **1987**, 1341.
(27) Abersfelder, K.; Nguyen, T.-l.; Scheschkewitz, D. *Z. Anorg. Allg. Chem.* **2009**, *635*, 2093.
(28) Nguyen, T.-l.; Scheschkewitz, D. *J. Am. Chem. Soc.* **2005**, *127*, 10174.
(29) For example, see: (a) Pang, Y.; Li, J.; Hu, B.; Karasz, F. E. *Macromolecules* **1999**, *32*, 3946. (b) Yang, J.-S.; Liau, K.-L.; Li, C.-Y.; Chen, M.-Y. *J. Am. Chem. Soc.* **2007**, *129*, 13183.

Scheme 5. Syntheses of *p*-**7** and *m*-**7** (Tip = 2,4,6-$^{i}Pr_3C_6H_2$)

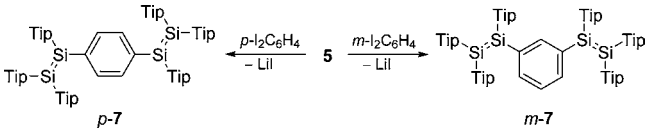

as yellow plates in two crops with a combined yield of 85%. The *m*-phenylene-bridged isomer *m*-**7** was fully characterized by multinuclear NMR and UV−vis spectroscopy and single-crystal X-ray diffraction.

The ^{29}Si NMR data for *m*-**7** are very similar to those for *p*-**7** (Table 1). The one-bond coupling constant between the silicon atoms [^{1}J(Si,Si) = 148.4 Hz] is marginally smaller than that of *p*-**7**, suggesting a somewhat weaker Si═Si bond, possibly as a result of increased steric repulsion. The ^{1}H and ^{13}C data confirmed the *m*-phenylene connectivity. The UV−vis spectrum quantified the initial visual impression that *m*-**7** exhibits a much smaller red shift of the longest-wavelength absorption than does *p*-**7** with respect to phenyldisilene **6a** (*m*-**7**, $\Delta\lambda_{max}$ = 11 nm; *p*-**7**, $\Delta\lambda_{max}$ = 69 nm). The non-negligible red shift still present may well be attributed to the structural effects of the increased steric interactions due to the closer proximity of the disilenyl groups.

The solid-state structure of *m*-**7** (Figure 4) indeed revealed significantly greater trans bending of the substituents than in *p*-**7** (Table 1) and Si−Si double bonds with lengths of 2.1914(9) and 2.1861(9) Å, which are thus considerably longer than the Si═Si bond in *p*-**7**. On the basis of the linear correlation derived from phenyldisilenes **6a**−**d** and *p*-**7** (Figure 3), however, ∼0.01 Å of these bond lengths can be attributed to the increased steric interaction in *m*-**7**. The greater steric strain between the two disilenyl units in *m*-**7** versus *p*-**7** is also expressed in slightly larger torsion angles of the Si═Si units with respect to the phenylene linker [Si2−Si1−C91−C96 = −44.0(2)° and Si4−Si3−C93−C94 = −47.6(2) in *m*-**7** vs Si2−Si1−C1−C3 41.0(2)° in *p*-**7**; Figure 5]. Nonetheless, the difference in dihedral distortions is not large enough to explain the absence of significant conjugation in *m*-**7**, and therefore, the electronic nature of the linking unit appears to be the sole determining factor. In order to corroborate this assertion, we carried out cyclic voltammetry studies on both *m*-**7** and *p*-**7**.

2.5. Electrochemical and EPR Studies of *m*-7 and *p*-7. The redox behavior of *m*-**7** and *p*-**7** was studied using cyclic voltammetry (CV) in THF under strictly anaerobic and anhydrous conditions. The potentials were referenced against the ferrocene/ferrocenium (Fc/Fc^{+}) couple. Both *m*-**7** and *p*-**7** display irreversible oxidation processes centered at E_{pa} = −0.14 V for *m*-**7** and E_{pa} = −0.35 V for *p*-**7** (for full CV scans, see the Supporting Information). In contrast to the reported cyclic voltammograms of $Tip_2Si{=}SiTip_2$ (**12**; $E^0_{1/2}$ = +0.56; +1.32 V vs Fc/Fc^{+}),[30] both phenylene-bridged tetrasiladienes show only one oxidation wave shifted significantly toward cathodic potentials. Notably, the oxidation of *m*-**7** is slightly less cathodically shifted (i.e., *p*-**7** is easier to oxidize), in agreement with an increase in HOMO energy due to conjugation effects. Unlike the case of **12**, which exhibits only one reduction wave at $E^0_{1/2}$ = −2.66 V, we observed in each case two well-separated quasi-reversible reduction waves centered at $E^0_{1/2}(1)$ = −2.70 and $E^0_{1/2}(2)$ = −3.30 V for *m*-**7** (Figure S18 in the Supporting Information) and $E^0_{1/2}(1)$ = −2.70 and $E^0_{1/2}(2)$ = −3.02 V for *p*-**7** (Figure 6).

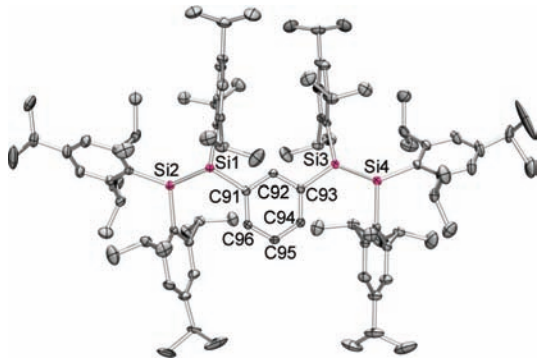

Figure 4. Solid-state structure of *m*-phenylene-bridged tetrasiladiene *m*-**7**. Hydrogen atoms, alternative positions of disordered isopropyl groups, and the 3.5 molecules of benzene have been omitted for clarity.

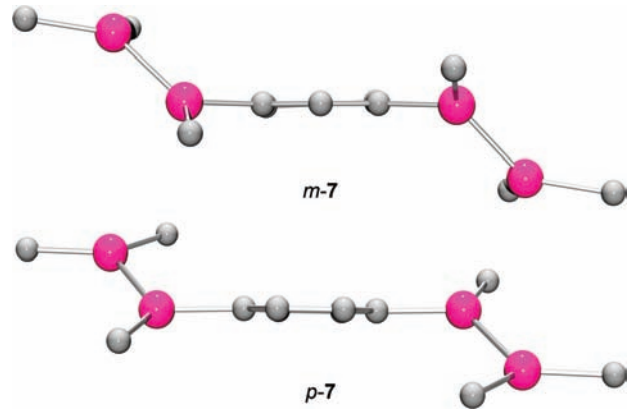

Figure 5. Side views of simplified solid-state structures of (top) *m*-**7** and (bottom) *p*-**7**.

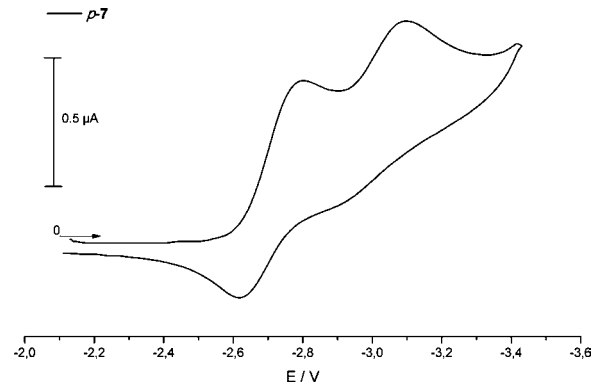

Figure 6. Cyclic voltammogram of *p*-**7** at room temperature in THF vs the Fc/Fc^{+} couple obtained using a scan rate 200 mV s^{-1} and Pt/[*n*Bu$_4$N][PF$_6$]/Ag. Both redox waves showed completely the same behavior in a second CV cycle; only one cycle is shown here. One irreversible oxidation process centered at E_{pa} = −0.35 V is not shown for clarity (see the Supporting Information).

The second reduction of *m*-**7** is very close to the cathodic limit of the redox window of the solvent and hence must be treated with some caution. The invariance of the first reduction wave, however, suggests that the presumably silicon-centered reductions are almost independent of conjugative effects. The differences in the peak potentials, $\Delta\varphi_p = \varphi_p^a - \varphi_p^c$, for the two compounds and each reduction step were revealed to be $\Delta\varphi_p(1)$ = 0.17 V and $\Delta\varphi_p(2)$ = 0.15 V for *p*-**7** and $\Delta\varphi_p(1)$ =

(30) Kira, M.; Ishima, T.; Iwamoto, T.; Ichinohe, M. *J. Am. Chem. Soc.* **2001**, *123*, 1676.

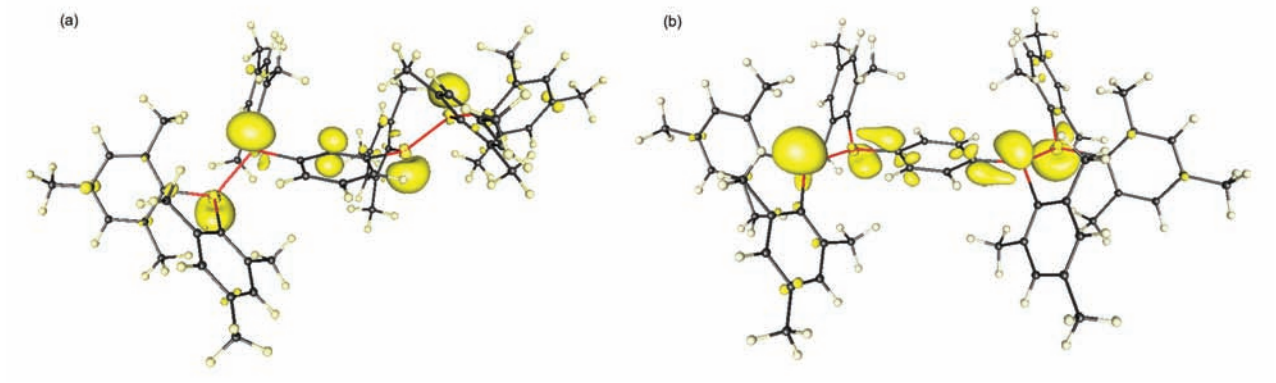

Figure 7. DFT-calculated spin densities for (a) [*m*-**7q**]$^{\bullet-}$ and (b) [*p*-**7q**]$^{\bullet-}$. Color code: silicon, red; carbon, gray; hydrogen, pale-yellow. Only positive spin density is shown.

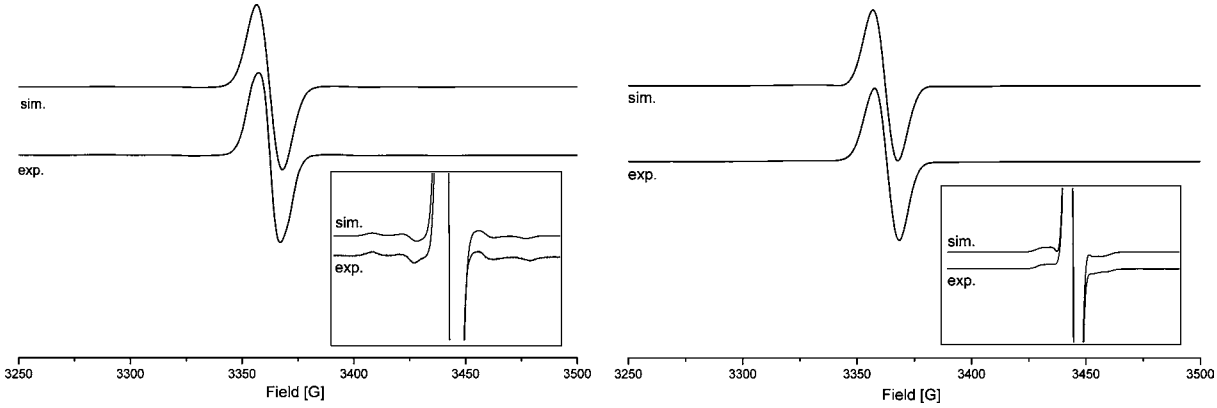

Figure 8. Experimental (exp.) and simulated (sim.) X-band CW EPR spectra of (left) [*m*-**7**]$^{\bullet-}$ [$g_{||} = 2.0064$, $g_{\perp} = 2.0057$, $A_{||}$(Si1) = 155 G, $A_{\perp}$(Si1) = 69 G, $A_{||}$(Si2) = 145 G, $A_{\perp}$(Si2) = 65 G] and (right) [*p*-**7**]$^{\bullet-}$ [$g_{||} = 2.0062$, $g_{\perp} = 2.0058$, $A_{||}$(Si1) = 90 G, $A_{\perp}$(Si1) = 38 G, $A_{||}$(Si2) = 72 G, $A_{\perp}$(Si2) = 32 G] in THF (frozen solution, 100 K). Insets: satellite signals due to couplings to the ^{29}Si nuclei.

0.50 V and $\Delta\varphi_p(2) = 0.15$ V for *m*-**7**. Because of the notably different electron-transfer kinetics for the first reduction of *m*-**7**, it is reasonable to assume a distinctive structural change upon one-electron reduction of *m*-**7**.[31] This suggestion was supported by density functional theory (DFT) calculations at the BP86/def2-TZVP level conducted on slightly modified model radical anions [*m*/*p*-**7q**]$^{\bullet-}$ featuring mesityl (Mes =2,4,6-$Me_3C_6H_2$) instead of Tip substituents on the Si atoms (Figure 7).

The most obvious difference between the two optimized structures is that [*p*-**7q**]$^{\bullet-}$ adopts an almost coplanar arrangement of the two Si═Si units and the *p*-phenylene bridge (torsion angles of 8.0 and 7.8°) whereas in [*m*-**7q**]$^{\bullet-}$ the Si═Si bonds are severely twisted out of the plane of the *m*-phenylene bridge (54.6 and 55.9°). In contrast, in the calculated structures of the neutral precursors *p*-**7q** and *m*-**7q**, the corresponding torsion angles are very similar, reiterating the experimental observations for *m*/*p*-**7** [*p*-**7q**, 19.9 and 20.0°, Δ(neutral/anion) = 11.9 and 12.2°; *m*-**7q**, 23.4 and 24.0°, Δ(neutral/anion) = 31.2 and 31.9°]. Obviously, the one-electron reduction of *m*-**7** incurs a considerably larger distortion of the molecular structure, nicely corroborating the interpretation of the electrochemical findings. This seems to be in line with the expected more efficient delocalization of the negative charge in the *p*-phenylene-linked [*p*-**7q**]$^{\bullet-}$. Consequently, the trans bending of [*p*-**7q**]$^{\bullet-}$ is slightly less pronounced than that of [*m*-**7q**]$^{\bullet-}$ ([*m*-**7q**]$^{\bullet-}$, $\theta = 30.5-34.5°$; [*p*-**7q**]$^{\bullet-}$, $\theta = 28.4-32.6°$). For both compounds, the Si═Si bonds are considerably elongated by 6.9 ([*p*-**7q**]$^{\bullet-}$) and 8.3 pm ([*m*-**7q**]$^{\bullet-}$) relative to the neutral precursors (*p*-**7q**, 2.176 Å; *m*-**7q**, 2.173 Å). Furthermore, the Si−C bonds to the phenylene bridge in [*p*-**7q**]$^{\bullet-}$ (1.853 Å) were revealed to be significantly shorter than in [*m*-**7q**]$^{\bullet-}$ (1.884 Å), indicating partial double bond character and therefore demonstrating the delocalization of the negative charge into the linking unit. This was further supported by spin density calculations (Figure 7), which showed a strong contribution of the ipso carbon atoms in the case of [*p*-**7q**]$^{\bullet-}$ but not for [*m*-**7q**]$^{\bullet-}$. Overall, however, the electron density in both radical anions is predominantly centered on the four silicon atoms (~44% for both [*m*-**7q**]$^{\bullet-}$ and [*p*-**7q**]$^{\bullet-}$).

A number of radical anions and one radical cation of disilenes with one Si═Si bond have been studied experimentally in the past.[3a,32] In order to support our computational findings by experiment, we thus performed electron paramagnetic resonance (EPR) measurements on frozen solutions of the in situ-generated radical anions at 100 K (Figure 8). [*m*/*p*-**7**]$^{\bullet-}$ gave strong, slightly axial symmetric signals with small satellites due to hyperfine coupling (hfc) to the ^{29}Si nuclei. The experimental spectra were successfully simulated using a system with $S = {}^1/_2$ and two different silicon atoms. The spin Hamiltonian parameters used for the simulation of [*m*-**7**]$^{\bullet-}$ are $g_{||} = 2.0064$ and $g_{\perp} = 2.0057$ with hfcs to two different ^{29}Si atoms ($I = {}^1/_2$) of $A_{||}$(Si1) = 155 G, $A_{\perp}$(Si1) = 69 G and $A_{||}$(Si2) = 145 G, $A_{\perp}$(Si2) = 65 G. The

(31) Geiger, W. E. *Organometallics* **2007**, *26*, 5738.
(32) (a) Weidenbruch, M.; Kramer, K.; Schäfer, A.; Blum, J. K. *Chem. Ber.* **1985**, *118*, 107. (b) Weidenbruch, M.; Thom, K.-L. *J. Organomet. Chem.* **1986**, *308*, 177. (c) Kira, M.; Iwamoto, T. *J. Organomet. Chem.* **2000**, *611*, 236. (d) Wiberg, N.; Niedermayer, W.; Polborn, K. *Z. Anorg. Allg. Chem.* **2002**, *628*, 1045. (e) Inoue, S.; Ichinohe, M.; Sekiguchi, A. *J. Am. Chem. Soc.* **2008**, *130*, 6078.

simulation for [*p*-**7**]$^{\bullet-}$, however, turned out to be challenging because the satellites were poorly resolved. A simulation with the spin Hamiltonian parameters $g_{\|} = 2.0062$ and $g_{\perp} = 2.0058$ and hfcs to two different ^{29}Si nuclei [$A_{\|}$(Si1) = 90 G, $A_{\perp}$(Si1) = 38 G and $A_{\|}$(Si2) = 72 G, $A_{\perp}$(Si2) = 32 G] nicely reproduced the line shape of the satellites of [*p*-**7**]$^{\bullet-}$. It is noteworthy that although the intensity of the satellites was slightly smaller than in the experimental spectra, other parameters did not furnish improved simulations. Nonetheless, the smaller hfcs of [*p*-**7**]$^{\bullet-}$ in comparison with [*m*-**7**]$^{\bullet-}$ are in line with the less pronounced trans bending in [*p*-**7**]$^{\bullet-}$ and hence a smaller s-orbital contribution within the Si═Si bonds (see above). Remarkably, the hfcs in the case of [*m*-**7**]$^{\bullet-}$ are significantly larger than that of the radical anion of disilene **1** with the sterically less demanding mesityl groups [A_{iso}(^{29}Si) = 49.6 G],[32a] implying larger trans bending despite the greater steric strain in [*m*/*p*-**7**]$^{\bullet-}$. Despite these gradual differences, however, all of the hfcs observed are consistent with a strongly predominant p character of the orbitals hosting the unpaired electron.[33] Overall, both EPR investigations nicely support the DFT calculations and the electrochemical findings by confirming the Si-centered nature of the reduction processes of the phenylene-bridged tetrasiladienes.

3. Conclusion

The transfer of Si═Si moieties to sterically innocent bromo- and iodoarenes using disilenide **5** is a powerful method for the synthesis of compounds with one or more Si═Si double bonds. The main conclusions of our study can be summarized as follows:

(1) The inertness of chloro and fluoro functionalities toward disilenide **5**, together with the absence of homocoupling products, favors a concerted aromatic substitution mechanism of the S_N2 type without, however, completely excluding the intermediate occurrence of radical pairs. Moreover, the low reactivity of **5** toward fluoro- and chlorobenzene raises the possibility of using these highly polar aromatics as solvents for reactions of disilenides.

(2) Residual halogen functionality at the para position is readily tolerated by disilenide **5**, opening the exciting perspective of functional group transformations in the presence of a Si═Si double bond. With the metal−halogen exchange reaction from **6d** to **6f**, we provided a first proof of principle for such a transformation.

(3) The (functionalized) phenyldisilenes **6a**−**d** exhibit a good (albeit not strong) correlation of the longest-wavelength UV−vis absorption with a modified electronic Hammett parameter that will be helpful in the deliberate tuning of HOMO−LUMO gaps of disilenes, although the cautionary note that only para substituents with similar electronic properties were analyzed must be added.

(4) The introduction of two Si═Si bonds was demonstrated for the *m*-phenylene-bridged derivative *m*-**7** in addition to the previously reported para isomer *p*-**7**.[13a] The conjugation mediated by the para linkage in *p*-**7** was corroborated by the absence of a significant red shift relative to phenyldisilene **6a** in the case of *m*-**7**. In addition, the presence of conjugation was lent support by electrochemical studies on *m*/*p*-**7** and EPR investigations on in situ-generated radical anions [*m*/*p*-**7**]$^{\bullet-}$, which were further elucidated by DFT calculations on slightly modified model systems.

(5) On the basis of the set of solid-state structures of disilenes with comparable steric congestion that is now available, the interrelated parameters of the Si═Si bond length and the trans-bent angles were satisfactorily correlated for the first time. A pseudolinear relationship was established that can be used as an approximate gauge of the degree of steric or electronic perturbation in compounds featuring the Tip_2Si═Si(Tip) moiety.

We have certainly barely scratched the surface of the inherent preparative possibilities of the Si═Si transfer reaction using disilenide **5**. There can be little doubt that the availability of a general protocol for the transfer of silicon−silicon double bonds will contribute to the firm establishment of the Si═Si moiety as a useful functional group and potent chromophore.

4. Experimental Section

General. All of the manipulations were carried out under a protective atmosphere of argon using standard Schlenk techniques or in a drybox. Ethereal solvents were refluxed over sodium/benzophenone and pentane, hexane, and (deuterated) benzene over sodium/potassium alloy; toluene was refluxed over sodium. All of the solvents were distilled and stored under argon and degassed prior to use. Tip_2Si═Si(Tip)Li (**5**) was prepared following our published procedure.[11a] Iodo- and diiodobenzenes were purchased from Aldrich, checked for purity by NMR analysis prior to use, and distilled or sublimed when necessary. The NMR spectra were recorded on a Bruker AV 500 or AV 400 FT-NMR spectrometer. ^{1}H and ^{13}C{^{1}H} NMR spectra were referenced to external tetramethylsilane (TMS) via the residual protons of the deuterated solvent (^{1}H) or the solvent itself (^{13}C). ^{29}Si{^{1}H} NMR spectra were referenced to external TMS and ^{19}F{^{1}H} NMR spectra to external $CFCl_3$. UV−vis spectra were recorded on Shimadzu UV Mini 1240 and PerkinElmer Lambda 25 spectrophotometers. Melting points were determined in closed NMR tubes under argon and are uncorrected.

General Procedure for the Preparation of Phenyldisilenes 6a−e,g and Bis(disilenyl)benzenes *m*-7 and *p*-7. Via cannula, a solution of the required stoichiometric amount of disilenide in 20 mL of benzene was added dropwise to a solution of 1.17 mmol of the appropriate iodobenzene (bromobenzene in the case of **6g**) in 15 mL of benzene at room temperature. After the mixture was stirred for 1 h at room temperature, the solvent was distilled off under vacuum. Hexane (35 mL) was added and the lithium halide separated from the solution by filtration. Crystallization at room temperature from a minimum amount of the indicated solvent afforded the corresponding product.

1-Phenyl-1,2,2-(2′,4′,6′-triisopropylphenyl)disilene (6a).[13a] Bright-yellow crystals from hexane, 0.50 g (58%, mp 156−157 °C, dec.). ^{1}H NMR (500.1 MHz, C_6D_6, 298 K): δ 7.38 (d, 2H, *o*-Ph-*H*), 7.12, 7.09, 7.04 (each s, each 2H, Tip-*H*), 6.92 (pseudo-t, 1H, *p*-Ph-*H*), 6.83 (pseudo-t, 2H, *m*-Ph-*H*), 4.29, 4.24 (each hept, each 2H, ^{i}Pr-C*H*), 4.03 (br., 2H, ^{i}Pr-C*H*), 2.76, 2.75, 2.70 (each hept, each 1H, ^{i}Pr-C*H*), 1.21, 1.19, 1.18, 1.15, 1.13, 1.11 (br.), 1.06 (each d, altogether 54H, ^{i}Pr-CH_3). ^{13}C NMR (125.1 MHz, C_6D_6, 298 K): δ 156.28, 155.72, 155.15, 151.72, 151.28, 150.73 (Tip-$C_{o/p}$), 138.67 (Ph-C_i), 136.30 (Ph-*C*H), 133.41, 133.13, 130.62 (Tip-C_i), 128.71, 128.06 (Ph-*C*H), 122.10, 122.06, 121.70 (Tip-*C*H), 38.43, 38.22, 37.57, 34.93, 34.76, 34.59 (^{i}Pr-*C*H), 25.68, 25.02 (br.), 24.69, 24.42 (br.), 24.32, 24.17, 24.01 (^{i}Pr-*C*H$_3$). ^{29}Si NMR (99.4 MHz, C_6D_6, 298 K): δ 71.8 (^1J(Si,Si) = 151.4 Hz, *Si*TipPh), 55.2 (^1J(Si,Si) = 151.4 Hz, *Si*Tip$_2$). UV−vis (hexane) λ_{max} (ε): 439 nm (19000 M^{-1} cm^{-1}). Exact mass (EI): found, 742.5331; calcd for $C_{51}H_{74}Si_2$, 742.5329.

1-(*p*-Fluorophenyl)-1,2,2-(2′,4′,6′-triisopropylphenyl)disilene (6b). Orange crystals from benzene, 0.77 g (86%, mp 143−145 °C, partial dec.). ^{1}H NMR (400.2 MHz, C_6D_6, 298 K): δ 7.32 (dd, 2H, Ph-H_o), 7.23, 7.19, 7.15 (each s, each 2H, Tip-*H*), 6.62 (dd, 2H, Ph-H_m), 4.30 (hept, 4H, ^{i}Pr-C*H*), 4.09 (hept, 2H, ^{i}Pr-C*H*), 2.85

(33) Review: Lee, Y. Va.; Sekiguchi, A. *Eur. J. Inorg. Chem.* **2005**, 1209.

(hept, 2H, ^{i}Pr-C*H*), 2.81 (hept, 1H, ^{i}Pr-C*H*), 1.31, 1.29, 1.27, 1.26, 1.21, 1.16 (each d, altogether 54H, ^{i}Pr-CH_3). ^{13}C NMR (100.6 MHz, C_6D_6, 298 K): δ 163.90 (^1J(C,F) = 248.8 Hz, Ph−C_p) 156.20, 155.73, 155.10, 151.88, 151.49, 150.84 (Tip-$C_{o/p}$), 138.20 (^3J(C,F) = 7.1 Hz, Ph-C_o), 134.21 (^4J(C,F) = 3.7 Hz, Ph-C_i) 133.19, 132.76, 130.45 (Tip-C_i), 122.12 (Tip-C_oH), 121.75 (Tip-C_pH), 115.30 (^{2}J(C−F) = 20.0 Hz, Ph-C_m), 38.45, 38.21, 37.61, 34.94, 34.76, 34.58 (^{i}Pr-*C*H), 25.64, 24.68, 24.32, 24.15, 23.99 (^{i}Pr-*C*H_3). ^{19}F{^{1}H} NMR (376.8 MHz, C_6D_6, 298 K): δ −111.51. ^{29}Si NMR (79.5 MHz, C_6D_6, 298 K): δ 70.6 (*Si*Ph), 55.7 (*Si*Tip). UV−vis (hexane) λ_{max} (ε): 437 nm (16800 M^{-1} cm^{-1}). Exact mass (EI): found, 760.5228; calcd for $C_{51}H_{73}Si_2F$, 760.5235.

1-(*p*-Chlorophenyl)-1,2,2-(2′,4′,6′-triisopropylphenyl)disilene (6c). Orange crystals from hexane, 0.43 g (47%, mp 145−147 °C, partial dec.). ^{1}H NMR (500.1 MHz, C_6D_6, 298 K): δ 7.25 (d, 2H, Ph-H_m), 7.22, 7.18, 7.14 (each s, each 2H, Tip-*H*), 6.92 (d, 2H, Ph-H_o), 4.27 (hept, 4H, ^{i}Pr-C*H*), 4.07 (hept, 2H, ^{i}Pr-C*H*), 2.85 (hept, 2H, ^{i}Pr-C*H*), 2.80 (hept, 1H, ^{i}Pr-C*H*), 1.31, 1.30, 1.29, 1.24, 1.23, 1.20, 1.15 (each d, altogether 54H, ^{i}Pr-CH_3). ^{13}C NMR (125.8 MHz, C_6D_6, 298 K): δ 156.28, 155.72, 155.15, 151.94, 151.62, 150.92 (Tip-$C_{o/p}$), 137.45 (Ph-$C_{p/i}$/Tip-C_i), 137.37 (Ph−C_o), 134.97, 133.04, 132.66, 130.10 (Ph-$C_{p/i}$/Tip-C_i), 128.35 (Ph-C_m), 122.15, 121.77 (Tip-C_m), 38.46, 38.29, 37.58, 34.94, 34.77, 34.58 (^{i}Pr-*C*H), 25.67, 24.69, 24.31, 24.15, 23.98 (^{i}Pr-*C*H_3). ^{29}Si NMR (99.4 MHz, C_6D_6, 298 K): δ 69.3 (*Si*Ph), 57.3 (*Si*Tip). UV−vis (hexane) λ_{max} (ε): 445 nm (19200 M^{-1} cm^{-1}). Exact mass (EI): found, 776.4935; calcd for $C_{51}H_{73}Si_2Cl$, 776.4939.

1-(*p*-Bromophenyl)-1,2,2-(2′,4′,6′-triisopropylphenyl)disilene (6d). Orange crystals from hexane, 0.22 g (23%, mp 143−145 °C, dec.). ^{1}H NMR (500.1 MHz, C_6D_6, 298 K): δ 7.22, 7.19 (each s, each 2H, Tip-*H*), 7.18 (d, 2H, Ph-H_m), 7.14 (s, 2H, Tip-*H*), 7.07 (d, 2H, Ph-H_o), 4.28 (hept, 4H, ^{i}Pr-C*H*), 4.08 (hept, 2H, ^{i}Pr-C*H*), 2.85 (hept, 2H, ^{i}Pr-C*H*), 2.80 (hept, 1H, ^{i}Pr-C*H*), 1.31, 1.29, 1.28, 1.23, 1.23, 1.20, 1.16 (each d, altogether 54H, ^{i}Pr-CH_3). ^{13}C NMR (125.8 MHz, C_6D_6, 298 K): δ 156.29, 155.72, 155.15, 151.97, 151.66, 150.94 (Tip-$C_{o/p}$), 137.89 (Ph-C_p), 137.63 (Ph-C_o), 133.01, 132.64 (Ph-C_i/Tip-C_i), 131.21 (Ph-C_m), 130.02, 123.39 (Ph-C_i/Tip-C_i), 122.16, 121.78 (Tip-C_m), 38.47, 38.30, 37.58, 34.92, 34.75, 34.57 (^{i}Pr-*C*H), 25.67, 24.68, 24.29, 24.15, 24.13, 23.96 (^{i}Pr-*C*H_3). ^{29}Si NMR (99.4 MHz, C_6D_6, 298 K): δ 69.2 (*Si*Ph), 57.4 (*Si*Tip$_2$). UV−vis (hexane) λ_{max} (ε): 447 nm (16200 M^{-1} cm^{-1}). Exact mass (EI): found, 820.4425; calcd for $C_{51}H_{73}Si_2Br$, 820.4434.

1-(*p*-Trimethylsilylphenyl)-1,2,2-(2′,4′,6′-triisopropylphenyl)disilene (6g). ^{1}H NMR (400.1 MHz, C_6D_6, 298 K): δ 7.40 (d, 2H, Ph-H_o), 7.14, 7.10 (each s, each 2H, Tip-*H*), 7.07 (d, 2H, Ph-H_m), 7.05 (s, 2H, Tip-*H*), 4.32 (hept, 2H, ^{i}Pr-C*H*), 4.22 (hept, 2H, ^{i}Pr-C*H*), 4.03 (hept, 2H, ^{i}Pr-C*H*), 2.76 (hept, 2H, ^{i}Pr-C*H*), 2.71 (hept, 1H, ^{i}Pr-C*H*), 1.23, 1.20, 1.28, 1.18, 1.17, 1.14, 1.10, 1.07 (each d, altogether 54H, ^{i}Pr-CH_3). ^{13}C NMR (100.6 MHz, C_6D_6, 298 K): δ 156.29, 155.74, 155.10 (Tip-C_o), 151.70, 151.28, 150.70 (Tip-C_p), 140.54 (Ph-C_i), 139.20 (Ph-C_p), 135.46 (Ph-C_o), 133.55, 133.24 (Tip-C_i), 132.89 (Ph-C_m), 130.56 (Tip-C_i), 122.09, 121.65 (Tip-C_m), 38.50, 38.16, 37.63, 34.94, 34.75, 34.59 (^{i}Pr-*C*H), 25.74, 24.70, 24.34, 24.17, 24.03 (^{i}Pr-*C*H_3), −1.24 (Si*Me*$_3$). ^{29}Si NMR (79.5 MHz, C_6D_6, 298 K): δ 71.5 (*Si*Ph), 56.5 (*Si*Tip$_2$), −4.6 (*Si*Me$_3$). Exact mass (EI): found, 814.5718; calcd for $C_{54}H_{82}Si_3$, 814.5724.

1,3-Bis[1′,2′,2′-tris(2″,4″,6″-triisopropylphenyl)disilenyl]benzene (*m*-7). Orange crystals from benzene, 0.76 g (39%, mp 162 °C). From the mother liquor, up to 0.90 g (46%) of somewhat impure additional product was obtained. ^{1}H NMR (500.1 MHz, C_6D_6, 298 K): δ 7.52 (s, 1H, Ph-$H_{(2)}$), 7.09 (d, 2H, Ph-$H_{(4,6)}$), 7.08 (s, 4H, Tip-*H*), 6.99, 6.97 (each s, each 4H, Tip-*H*), 6.49 (t, 1H, ^1J(H,H) = 7.50 Hz, Ph-$H_{(5)}$), 4.11, 4.07 (each hept, each 4H, ^{i}Pr-C*H*), 3.83 (hept, 4H, ^{i}Pr-C*H*), 2.75, 2.72 (each hept, each 2H, ^{i}Pr-C*H*), 2.66 (hept, 2H, ^{i}Pr-C*H*), 1.24, 1.22, 1.14, 1.10, 0.98, 0.90 (each d, altogether 108H, ^{i}Pr-CH_3). ^{13}C NMR (125.1 MHz, C_6D_6, 298 K): δ 156.10, 155.67, 154.89 (Tip-C_o), 151.32, 151.19, 150.40 (Tip-C_p), 142.00 (Ph-$C_{(2)}$H), 137.84 (Ph-C_i), 136.41 (Ph-$C_{(4,6)}$H), 133.91, 133.52, 129.77 (Tip-C_i), 127.67 (Ph-$C_{(5)}$H), 122.10, 121.47 (Tip-*C*H), 38.46, 37.99, 37.54, 34.92, 34.77, 34.48 (^{i}Pr-*C*H), 26.12, 25.85, 24.55, 24.22, 24.17, 23.97 (^{i}Pr-*C*H_3). ^{29}Si NMR (99.4 MHz, C_6D_6, 298 K): δ 72.9 (^1J(Si,Si) = 148.4 Hz, *Si*TipPh), 54.6 (^1J(Si,Si) = 148.4 Hz, *Si*Tip$_2$). UV−vis (hexane) λ_{max} (ε): 450 nm (39000 M^{-1} cm^{-1}). MS (EI) *m*/*z* (%): 1407.9 (M^+, 10), 1267.7 (10), 1194.8 (20), 1176.8 (30), 1062.5 (85), 1021.5 (55), 1007.6 (25), 989.6 (10), 859.3 (10), 817.3 (10), 451.3 (100), 433.3 (80). Anal. Calcd for $C_{96}H_{142}Si_4$: C, 81.86; H, 10.16. Found: C, 79.21; H, 9.85. Deviation likely due to the high oxygen sensitivity of *m*-**7** (calcd for $C_{96}H_{142}Si_4O_3$: C, 79.16; H, 9.83).

1,4-Bis[1′,2′,2′-tris(2″,4″,6″-triisopropylphenyl)disilenyl]benzene (*p*-7).[13a] Red crystals from pentane, 1.20 g (72%, mp 190 °C, dec.). ^{1}H NMR (500.1 MHz, C_6D_6, 298 K): δ 7.11, 7.06, 7.03 (each s, each 4H, Tip-*H*), 6.84 (s, 4H, −C_6H_4−), 4.18, 4.13, 3.94, 2.76 (each hept, each 4H, ^{i}Pr-C*H*), 2.68 (hept, 2H, ^{i}Pr-C*H*), 1.24, 1.22, 1.18, 1.14 (br.), 1.12, 1.04 (each d, altogether 108H, ^{i}Pr-CH_3). ^{13}C NMR (125.1 MHz, C_6D_6, 298 K): δ 156.31, 155.54, 155.09, 151.48, 151.31, 150.58 (Tip-$C_{o/p}$), 139.14 (C_6H_4-C_i), 134.75 (Ph-*C*H), 133.59, 133.37, 130.16 (Tip-C_i), 128.59 (C_6H_6), 122.15, 122.06, 121.60 (Tip-*C*H), 38.29, 38.10, 37.38, 34.94, 34.81, 34.53 (^{i}Pr-*C*H), 25.95, 25.19 (br.), 24.71, 24.41, 24.29, 24.19, 23.98 (^{i}Pr-*C*H_3). ^{29}Si NMR (99.36 MHz, C_6D_6, 298 K): δ 70.7 (^1J(Si,Si) = 150.0 Hz, *Si*Tip), 56.8 (^1J(Si,Si) = 150.0 Hz, *Si*Tip$_2$). UV−vis (hexane) λ_{max} (ε): 508 nm (27000 M^{-1} cm^{-1}). MS (EI) *m*/*z* (%): 1407.9 (M^+, 15), 1176.8 (100), 1062.5 (40), 1021.5 (20), 945.6 (15), 492.2 (20), 451.2 (15), 433.3 (70). A satisfactory elemental analysis could not be obtained, presumably because of the high oxygen sensitivity.

Lithiation of 6d with ^{t}BuLi To Afford 6f. A pentane solution of ^{t}BuLi (0.71 mL, 1.7M) was added dropwise via syringe within 10 min to a stirred solution containing 0.50 g (0.61 mmol) of **6d** in 15 mL of Et_2O at −75 °C. The mixture was stirred for 2 h at −75 °C, allowed to warm to −50 °C within 1 h, kept at this temperature for 10 min, and then cooled again to −75 °C. Me_3SiCl was added dropwise over the course of 5 min via syringe, after which the reaction mixture was very slowly (10 °C/h) brought back to room temperature. Solvents and volatiles were removed under vacuum, after which hexane was added and the lithium salts filtered off. Removal of hexane under vacuum afforded a mixture of **6g** and **6a** according to NMR spectroscopic data (in different runs, **6g**/**6a** ratios between 8:2 and 9:1 were obtained).

Crystallography. Single crystals of **6b**−**d** and *m*-**7** were coated with perfluorinated polyether and transferred to the cold nitrogen stream at the goniometer. Data were collected on a Bruker Smart Apex II (*m*-**7**), Oxford Diffraction Xcalibur PX Ultra (**6b** and **6c**), or Oxford Diffraction Xcalibur 3 (**6d**) diffractometer. The cells were determined accurately on a representative set of frames. Data reduction was carried out with SAINT+ version 6.22 (*m*-**7**), CrysAlis Pro version 1.171.33.48 (**6b** and **6c**), or CrysAlis Pro version 1.171.33.41 (**6d**). Semiempirical absorption corrections were applied to the data for *m*-**7** using SADABS, while analytical absorption corrections were applied to the data for **6b** and **6c** using CrysAlis Pro version 1.171.33.48 and to the data for **6d** using CrysAlis Pro version 1.171.33.41. Refinement proceeded smoothly to yield the crystallographic parameters summarized in Table 2. The absolute structure of **6b** was shown to be a partial racemic twin by a combination of *R*-factor tests [R_1^+ = 0.0472, R_1^- = 0.0507] and by use of the Flack parameter [x^+ = +0.167(11), x^- = +0.833(11)].

Cyclic Voltammetry. Cyclic voltammetry measurements were performed with an EG&G potentiostat (PAR model 263A) and an electrochemical cell for sensitive compounds.[34] We used a freshly polished Pt disk working electrode, a Pt wire as the counter electrode, and a Ag wire as the (pseudo)reference electrode; [nBu$_4$N][PF$_6$] (0.1 M) was used as the electrolyte. Potentials were calibrated against the Fc/Fc$^+$ couple (internal standard), which has a potential of $E^0_{1/2}$ = 0.35 V versus Ag/AgCl.

(34) (a) Hinkelmann, K.; Heinze, J.; Schacht, H.-T.; Field, J. S.; Vahrenkamp, H. *J. Am. Chem. Soc.* **1989**, *111*, 5078. (b) Heinze, J. *Angew. Chem.* **1984**, *96*, 823; *Angew. Chem., Int. Ed. Engl.* **1984**, *23*, 831.

Table 2. Selected Crystallographic Details for Compounds **6b−d** and *m*-**7**

	6b	**6c**	**6d**	*m*-**7** · $3.5C_6H_6$
formula	$C_{51}H_{73}FSi_2$	$C_{51}H_{73}ClSi_2$	$C_{51}H_{73}BrSi_2$	$C_{117}H_{163}Si_4$
T (K)	173(2)	173(2)	173(2)	173(2)
λ (Å)	1.54184	1.54184	0.71073	0.71073
color, habit	yellow, block	orange, block	orange, block	yellow, plate
crystal system	monoclinic	monoclinic	monoclinic	triclinic
space group	$P2_1$	$P2_1/c$	$P2_1/c$	$P\bar{1}$
a (Å)	15.38356(8)	18.55902(9)	18.5602(3)	10.2487(7)
b (Å)	16.80979(9)	12.81965(5)	12.84960(16)	21.6060(15)
c (Å)	37.8732(2)	21.65869(9)	21.6993(3)	26.9115(2)
α (deg)	90	90	90	68.187(2)
β (deg)	100.2271(5)	109.6339(5)	109.5139(16)	81.340(2)
γ (deg)	90	90	90	82.160(2)
V (Å^3)	9638.19(9)	4853.43(3)	4877.84(13)	5448.3(7)
Z	8	4	4	2
d (g cm^{-3})	1.049	1.064	1.120	1.025
μ (mm^{-1})	0.919	1.386	0.923	0.099
F(000)	3328	1696	1768	1842
θ_{max} (deg)	72.58	72.47	31.97	25.03
total reflns	73962	55005	43582	43080
unique reflns	36582	9592	14784	19141
reflns with $I > 2\sigma$	33450	8423	8546	15398
R_{int}	0.0262	0.0263	0.0228	0.0510
restraints	439	63	57	60
parameters	2024	514	514	1326
S	1.045	1.086	0.909	1.107
R_1 ($I > 2\sigma$)	0.0470	0.0375	0.0357	0.0656
wR_2 (all data)	0.1272	0.1081	0.0895	0.1585

EPR Spectroscopy. Continuous wave (CW) EPR spectroscopy was performed at the X-band on a Bruker EMXplus spectrometer (microwave frequency 9.43 GHz) equipped with a liquid nitrogen cryostat. The spectra were measured with a modulation amplitude of 1 or 10 G and a modulation frequency of 100 kHz, and the field was calibrated by using 2,2-diphenyl-1-picrylhydrazyl (DPPH) with a g value of 2.0036. CW EPR simulations were calculated using the Bruker XSophe program package (version 1.1.4). In the simulations, we used the experimental central field and sweep width.

DFT Calculations. Calculations were performed with the TURBOMOLE program package.[35] The geometries were optimized without symmetry restrictions at the (RI)-BP86[36] level using def2-TZVP basis sets (see the Supporting Information).[37] The spin densities were calculated using the pointval module of TURBOMOLE. The spin density quantification was done using a home-written script. Because of the large number of atoms, analytical frequency calculations were not performed.

Acknowledgment. This work was supported by the DFG (Sche906/3-1 and 3-2), the Karl Winnacker-Fonds of the Aventis Foundation, the Gottlieb Daimler and Karl Benz Foundation, the EPSRC (EP/H048804/1), and in part by the Fonds der Chemischen Industrie. We thank Peter R. Haycock and Richard N. Sheppard for the acquisition of NMR spectra and Alexander Baldes for technical assistance.

Supporting Information Available: Crystallographic data for **6b−d** and *m*-**7** (CIF), NMR spectra, full cyclic voltammograms, and Cartesian coordinates of the DFT-calculated structures. This material is available free of charge via the Internet at http://pubs.acs.org.

JA107547S

(35) (a) *TURBOMOLE*, version 6.0; TURBOMOLE GmbH: Karlsruhe, Germany, 2009. TURBOMOLE was developed by the University of Karlsruhe (TH) and Forschungszentrum Karlsruhe GmbH from 1989−2007; since 2007, it is available at http://www.turbomole.com. (b) Ahlrichs, R.; Bär, M.; Häser, M.; Horn, H.; Kölmel, C. *Chem. Phys. Lett.* **1989**, *162*, 165. (c) Treutler, O.; Ahlrichs, R. *J. Chem. Phys.* **1996**, *102*, 346. (d) Sierka, M.; Hogekamp, A.; Ahlrichs, R. *J. Chem. Phys.* **2003**, *118*, 9136. (e) Ahlrichs, R. *Phys. Chem. Chem. Phys.* **2004**, *6*, 5119.

(36) (a) Slater, J. C. *Phys. Rev.* **1951**, *81*, 385. (b) Vosko, S. H.; Wilk, L.; Nusair, M. *Can. J. Phys.* **1980**, *58*, 1200. (c) Becke, A. D. *Phys. Rev. A* **1998**, *38*, 3098. (d) Perdew, J. P. *Phys. Rev. B* **1986**, *33*, 8822.

(37) (a) Weigend, F.; Ahlrichs, R. *Phys. Chem. Chem. Phys.* **2005**, *7*, 3297. (b) Weigend, F. *Phys. Chem. Chem. Phys.* **2006**, *8*, 1057.